Physicochem. Probl. Miner. Process., 62(1), 2026, 217567 | Physicochemical Problems of Mineral Processing

http://www.journalssystem.com/ppmp | ISSN 1643-1049

Numerical simulation and experimental study on jet- pipeline-drop plate combined flotation enhancement device

Zhou Wei [1,2], Wang Zilong [1], Wang Hui [1], Li Long [1]

[1] School of Materials Science and Engineering, Anhui University of Science and Technology, Huainan, Anhui 232001, China

[2] State Key Laboratory of Mining Response and Disaster Prevention and Control in Deep Coal Mines, Huainan 232001, China

Corresponding author: awaly@126.com (Wei Zhou)

Abstract: To address the demand for efficient pulp conditioning technology in coal slime flotation, this paper designs a combined pulp conditioning device based on jet mixing, pipeline mixing, and drop plate mixing. Through a combination of COMSOL numerical simulation and physical experiments, parameter optimization tests were conducted for each stage of jet, pipeline, and drop plate. The pulp conditioning effect was verified through flotation tests. The results indicate that when the ratio of the incident flow rate to the instantaneous mixing volume in the tank is 0.414, an optimal flow field is achieved in the tank for the mixing of reagents and pulp. Increasing the number of mixing units within the pipeline mixing enhances the turbulence intensity of the fluid, thereby further improving the contact probability between reagents and mineral particles. When the angle of the drop plate is set at 15°, particles are more evenly distributed on the baffle plate, which can increase the pretreatment time and enhance the effect of the baffle bars. Compared with the slurry flotation of 1.5 L single tank flotation machine, the flotation test was carried out on the slurry after the slurry was adjusted by the Jet - Pipeline - Drop plate combined slurry adjustment device. The yield of clean coal was increased by 6.85 %, and the recovery rate of clean coal combustible was increased by 8.85 %.

***Keywords*:** jet dispersion, drop mixing, pulp conditioning device, mechanism optimization

1. Introduction

The jet-pipeline-drop plate combined pulp conditioning device is a composite apparatus based on jet mixing, pipeline mixing, and drop plate mixing (Ma et al.2021; Xiao et al. 2012; Cheng et al. 2023; Yu et al. 2014; Zhang et al. 2021). It further diversifies the means of coal slime pulp conditioning compared to the traditional single-stirring method. This device has the application effects of increasing the contact probability between reagents and mineral particles, significantly enhancing mineralization efficiency, and improving the selectivity of coal slime flotation (Wei et al. 2016; Zhao 2023; Dai et al. 2023; Qu et al. 2023).

Pulp conditioning operation can remove the fine slime coating on the coal surface and increase the probability of reagent adsorption, making it an indispensable and crucial step before flotation. Many scholars have conducted in-depth research on efficient pulp conditioning methods. Wang et al. (2021) explored, through numerical simulation, the impact of the annular jet mixing zone on air suction effects and bubble closure characteristics, and analyzed the effects of different degrees of closure on air suction performance and the gas-liquid ratio. By employing high-speed dynamic imaging technology, they recorded the variations in bubble size, rise velocity, and gas content with changes in the degree of closure. As the degree of closure in the mixing zone increased, the inlet air jet could more effectively overcome the static pressure outside the nozzle. Wang et al. (2020) utilized Fluent software to simulate the flow field characteristics of an impinging jet pulp conditioning device and analyzed the variation patterns of hydrodynamic parameters. Their aim was to promote the mixing of particles and reagents through high-speed impingement, thereby enhancing the adsorption effect of reagents on the particle

DOI: 10.37190/ppmp/217567

surfaces. Wang et al. (2015), on the other hand, analyzed the impact of the variation in the spacing between the nozzle and the throat on the performance of a microbubble generator through a numerical model. It was found that within a certain range of spacing, when the water volume flow rate was fixed, the performance of the bubble generator reached its optimum. Within this range, an increase in air suction volume led to a decrease in bubble diameter and a more uniform bubble distribution, which was beneficial for the flotation of fine minerals. Zhu et al. (2009) employed the Computational Fluid Dynamics (CFD) method to investigate the influence of key geometric parameters on the performance of an ejector, such as the layout of the primary nozzle outlet and the convergence angle of the mixing section. Ansari et al. (2018) described the gas entrainment and bubble generation mechanisms of a novel micro-ejector. Han et al. (2023) explored the adsorption of reagents on the surface of coal slime particles in a jet-agitation coupled flotation device to enhance the modification effect of coal slime. Xu et al. (2020) proposed a combined column flotation process aimed at reducing the entrainment of coal gangue particles, thereby lowering the ash content of coal flotation concentrate. Zhou et al. (2020) designed two types of jet-agitation devices with different structural parameters. By adding guide vanes to improve the flow field, they enhanced the air suction capacity. Feng et al. (2018) developed a coal slime pulp conditioning device that integrates multiple mixing methods, achieving deep modification of coal slime. Wang et al. (2022) studied the effect of impinging jet pulp conditioning on the flotation performance of oxidized coal, while Li et al. (2022) analyzed the impact of jet mixers on the distribution of mineral elements in coal flotation products under different energy inputs. Gao et al. (2023) took the ZWF6500 jet micro-bubble flotation machine as an example and used CFD numerical simulation to study the influence of bubble generator structural parameters on physical parameters such as gas holdup. Zheng et al. (2022) explored, through numerical simulation, the impact of nozzle outlet shape on the velocity and impact pressure of water jets, and analyzed the variations in velocity and dynamic pressure at different distances.

This thesis proposes a combined jet-pipeline-drop pulp conditioning device that enhances the pulp conditioning effect for coal slime flotation through the synergistic interaction of three components: the jet, the pipeline mixer, and the drop plate. Numerical simulations were conducted to establish a physical model, analyze the jet-pipeline-drop interaction mechanism, and reveal the flow field characteristics and the inter-particle interaction mechanisms during jet entrainment, pipeline mixing, and the drop plate process. This research enriches the theoretical foundation of coal slime flotation pulp conditioning and provides an efficient technical solution for coal slime pulp conditioning.

2. Device design

2.1. Device structure and working principle

This device mainly consists of a tank body, a chemical dispersal system, a pipeline mixing unit, an inclined drop plate, and a false-bottom mixing unit. The two sets of jet mixing devices serve as the core of the reagent dispersion system, and their structure is illustrated in Fig. 1. Compared with traditional jet mixing devices, this device adopts a multi-nozzle structure, which is more conducive to the emulsification and dispersion of reagents. The inclined drop plate is equipped with baffle strips, enabling different pretreatment times based on the particle size.

During the operation of the pulp conditioning device, the flotation reagent is drawn in through the reagent suction pipeline of the jet device, mixed with clean water, and then ejected through the diffuser tube into the reagent dispersion tank, completing the initial dispersion process of the reagent. The overflow from this tank, along with the overflow from the slurry feed tank, enters the pipeline mixing for the first mixing stage. After that, the mixture flows onto the drop plate equipped with baffle strips. Due to different resistances encountered, low-ash coarse coal slime particles and high-ash fine coal slime particles experience different pretreatment (climbing) times. Subsequently, a mixing unit is employed again in the pipeline at the material discharge outlet to complete the final rectification and conditioning process.

2.2. Model construction and mesh generation

There are buffers between the three parts of the jet, the pipeline, and the drop plate, so they are not

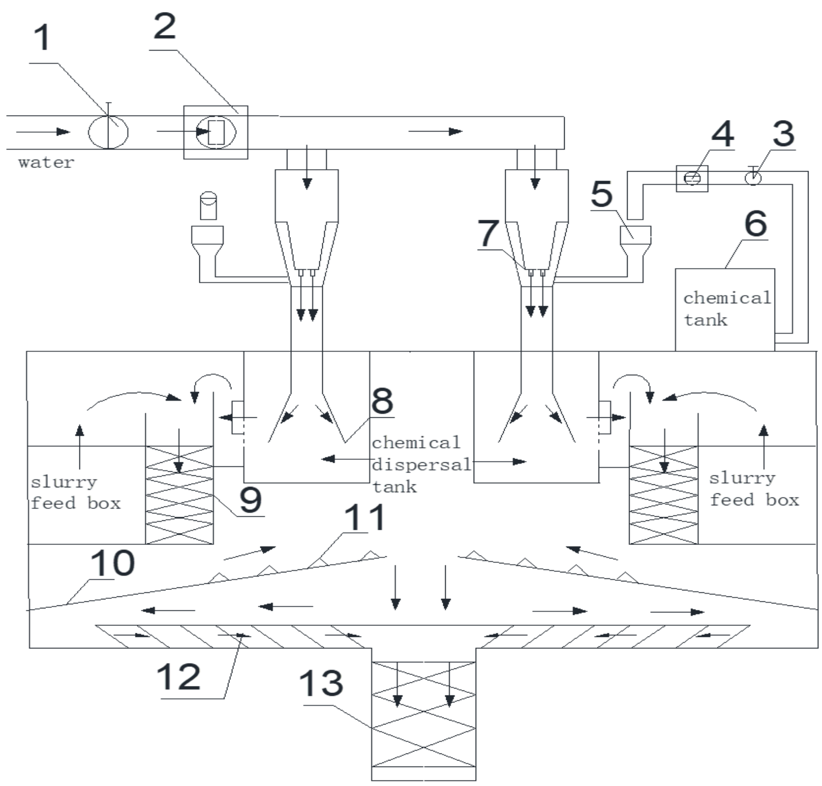

1,3-Control valves; 2,4-Flowmeters; 5-Reagent feeding funnel; 6-Reagent tank; 7-Multi-nozzle; 8-Ducted diffuser outlet; 9,13-Pipeline mixers; 10-Inclined drop plate; 11-Sill strip; 12-False bottom partition

Fig. 1. Diagram of the Jet-Pipeline-Drop plate combined pulp conditioning device

directly connected. Therefore, when conducting flow field simulation and analysis, separate models are established for each of the three components to simulate the flow field streamline distribution within each part individually.

Geometric modeling of each component of the jet-pipeline-drop plate combined pulp conditioning machine was carried out using SOLIDWORKS software. For the flow field simulation, the turbulent mixture model in the Fluid Flow module of COMSOL Multiphysics was selected, with the gravitational acceleration defined as -g. The models of each part are illustrated in Fig. 2:

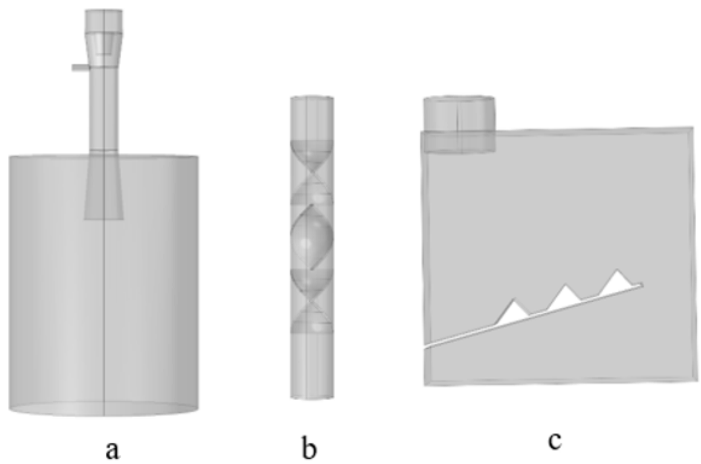

Fig. 2. Component models (a - Jet pipeline, b - pipeline mixer, c - drop plate)

Comsol's automatic mesh generation was employed to mesh each component. The jet pipeline unit had 383,501 mesh elements with an average mesh quality of 0.7023; the pipeline mixer unit had 139,297 mesh elements with an average mesh quality of 0.6565; and the drop box unit had 98,446 mesh elements with an average mesh quality of 0.6629. The parameters of each part of the device are shown in Table. 1.

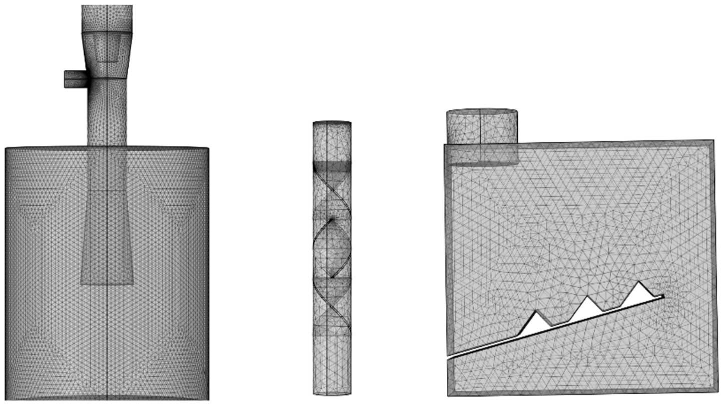

Fig. 3. Schematic diagram of mesh generation

Table. 1. Component parameters

Component	Parameter	Taken value
Jet pipeline	diameter of the feed pipe Dr/mm	30
	nozzle diameter Dz/mm	16.5
	convergence angle of the internal nozzle α/°	14
	area of the throat : area of the nozzle	2.69
	divergence angle β/°	9
	throat length : diffuser length	6:5
	throat diameter Dh/mm	23
	layout position of the suction tube	in the middle
	suction pipe diameter d1/mm	5
Pipeline mixer	diameter D/mm	25
	length L/mm	340
	internal static structure l/d	1.4
Drop plate	included angle θ/°	-15、0、15
	length Lb/mm	dependent on the working parameters
	number of turns	3

3. Flow field simulation and analysis

3.1. Analysis of jet mixing flow field

The distance between the bottom of the fixed jet pipe and the tank bottom is set at 150 mm, with an incident flow velocity of 1.5 m/s. An analysis and comparison are conducted on the velocity changes in the flow field, the three-dimensional motion distribution of streamlines, the characteristics of trailing vortices, and turbulent variables. This aims to explore the laws of fluid motion and particle dispersion mixing, as well as to determine the ratio of incident flow rate to the tank's instantaneous mixing volume that yields the optimal mixing of reagent and pulp. To investigate the optimal ratio of incident flow rate to the tank's instantaneous mixing volume (defined as b), three different ratio schemes are designed: b = 0.414, b = 0.225, and b = 0.144. The corresponding tank diameters for these ratios are 150 mm, 200 mm, and 250 mm, respectively.

The contour map of the diffusion velocity distribution of the jet flow is shown in Fig. 4, illustrating the changes in the velocity contour from 0.1 to 0.5 seconds when the incident flow velocity is 1.5 m/s.

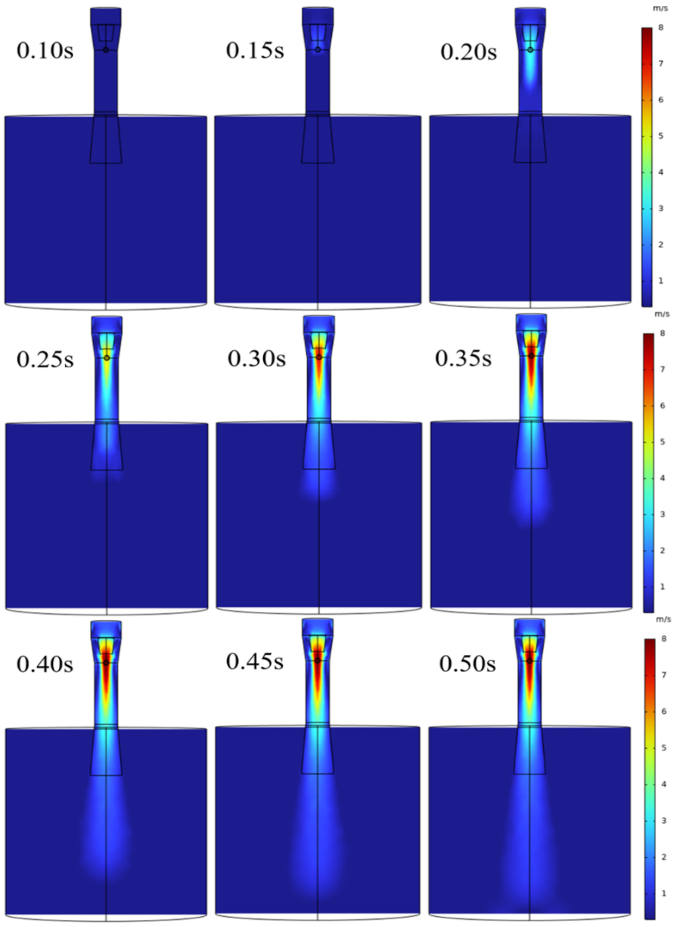

Fig. 4. Graph of velocity distribution changes in the flow field

As the fluid enters the nozzle, it is compressed, resulting in an increase in velocity, and reaches its maximum velocity within the throat chamber before undergoing deceleration. Using air as the carrier for the reagent, it enters the jet pipe and mixes with the pulp. The air outside the ejector tube is compressed into the interior due to negative pressure, where it collides with, cuts, and breaks up the fluid, and then together they enter the diffuser tube. The fluid at the outlet of the diffuser tube disperses throughout the tank. The fluid in the center is directed towards the bottom of the tank, where its velocity decreases and rises together with the accumulated fluid in the tank. As the diameter of the cylinder decreases, the flow velocity tends to increase, and there is still a relatively strong flow velocity at higher levels. The overall velocity distribution of the flow field's coherent motion is relatively balanced. From the figure, it can be observed that the fluid possesses a high jet velocity within the nozzle chamber, while the velocity of the fluid inside the tank increases, and the velocity in the overflow layer decreases and stabilizes at around 0.1 m/s.

A streamline motion trajectory diagram was created for the overall flow field to investigate the three-dimensional motion distribution and velocity of the fluid within the tank under different parameters, with arrows indicating the direction of motion. Fig. 5. illustrates the three-dimensional streamline distribution under varying cylinder diameters. When the cylinder diameter is 150 mm, the streamlines are relatively dense, but the fluid circulation zone is not fully developed. As the diameter increases, the circulation area expands but becomes more dispersed towards the sides, resulting in the existence of weak interaction zones in the space.

Fig. 6 presents the isosurface diagram of the trailing vortex structure under the jet mixing flow field. Judging from the vorticity magnitude, the vorticity within the jet pipe chamber is significantly greater than that distributed in the tank, indicating strong initial cross-vortex motion of the fluid in the jet pipe. As the cylinder diameter increases, the distribution pattern of vorticity changes. At 150 mm, there are more uniformly and densely dispersed vortices. At 200 mm, the vortices are more concentrated towards the outer side. At 250 mm, the vortices are divided into inner, middle, and outer circular zones centered around the jet pipeline, with relatively large spaces in between each layer. In the vertical direction, it can be observed that more layers of vortices are generated at 150 mm, with numerous and clustered tiny vortex clusters in the middle diffusion zone. The jet exhibits the maximum vorticity value at 200 mm and the minimum at 150 mm.

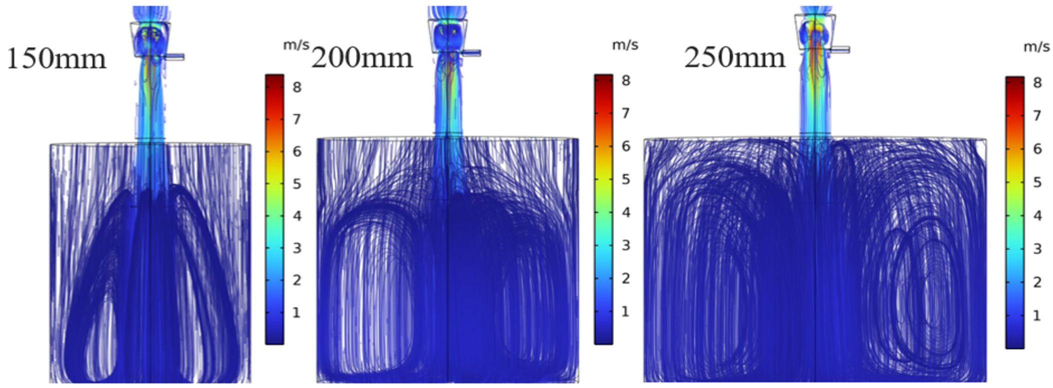

Fig. 5. Streamline distribution for different cylinder diameters

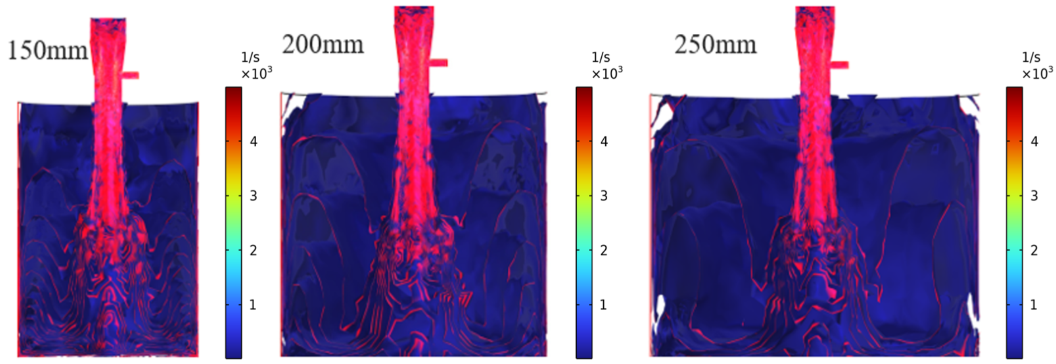

Fig. 6. Schematic diagram of vortex morphology

The turbulent dissipation rate describes the rate at which kinetic energy is converted into thermal energy through viscous effects during turbulent motion, and its influence on fluid mixing performance is complex and multidimensional. At small scales, vortices enhance microscopic mixing by promoting substance diffusion. A high dissipation rate can disrupt density stratification or concentration gradients, thereby reducing the mixing resistance caused by stratification. However, at large scales, vortices may not develop fully, leading to potential inhomogeneity in macroscopic mixing and the formation of dead zones.

From Fig. 7, it can be inferred that the flow (flow jet) morphology formed by the structural parameters of the jet pipeline primarily determines the turbulence intensity and the region of influence within the tank. Under this jet mixing mechanism, variations in the height and volume of the cylindrical section can have varying degrees of impact on the distribution of the turbulent flow field. The dissipation rate is relatively high within the jet chamber, and thus, an analysis of the dissipation effect is conducted by taking cross-sections of the tank.

Fig. 8 illustrates the distribution of turbulence intensity within the mixing tank at the Y=-200 cross-section under the influence of the turbulent flow field. The turbulent dissipation rate exhibits a normal distribution characteristic, with the cylinder having a diameter of 150 mm displaying the highest dissipation rates at both the peak and wall regions, while the dissipation rates for cylinders with diameters of 200 mm and 250 mm show a decrease. In each of the figures, the axial position where the turbulence values are relatively high is approximately around 80 mm. Based on the analysis and comparison of the three-dimensional motion distribution of streamlines, characteristics of trailing vortices, and turbulent variables, it is found that when the tank diameter is 150 mm (i.e., the ratio of the incident flow rate to the instantaneous mixing volume of the tank, denoted as b = 0.414), the tank exhibits an optimal flow field for the mixing of reagents and pulp.

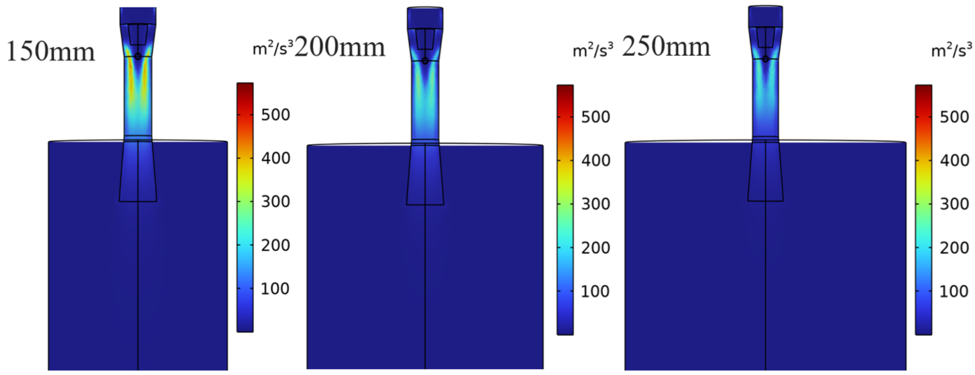

Fig. 7. Turbulent dissipation rate

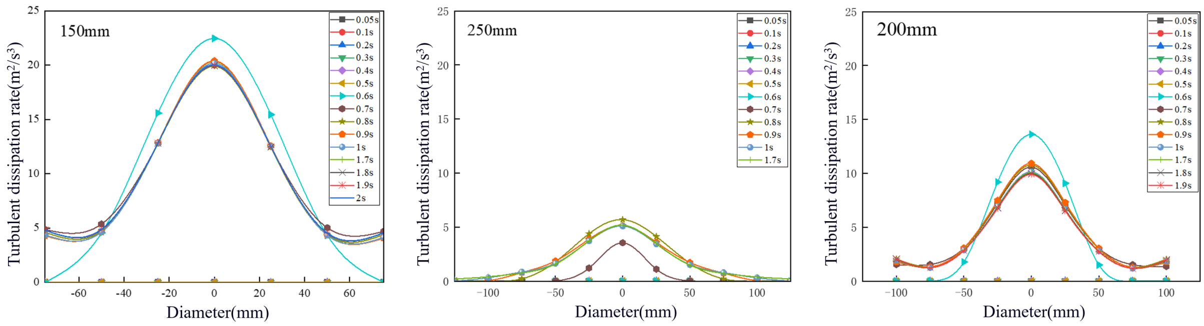

Fig. 8. Turbulent dissipation rate at Y = -200 mm

3.2. Numerical simulation of pipeline mixers

The velocity distribution of the flow field inside the pipeline mixer is illustrated in Fig. 9. It can be observed that during the steady flow process, the fluid velocity is higher in the central region due to the squeezing effect of the blades and the wall. The redirection of the fluid between the blades creates velocity differences, which enhance mixing. The maximum vortex flow occurs at the location where the rotation angle reaches its peak, consistent with the velocity distribution. Each vortex gradually dissipates towards the edges as it moves with the fluid, which also leads to further mixing and adhesion of the fluid layers due to the influence of small eddies. The positive and negative values of the numerical data reflect the opposite directions of fluid motion within the pipeline mixer, with the fluids colliding and dispersing among each other. As the number of mixing elements increases, the vorticity generated by the fluid also increases, thereby improving the mixing efficiency.

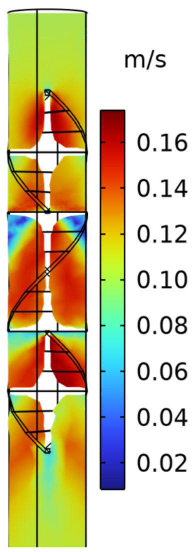

Fig. 9. Pipeline mixer velocity distribution cloud

The streamline distribution is depicted in Fig. 10. It can be observed that near the upper end of the blade and close to the wall, a portion of the fluid is cut off and collides with the wall, causing a sharp decrease in velocity for that part, while the fluid in immediate contact with it experiences a sudden increase in velocity. Additionally, small vortices are generated at the angles on the same blade surface. As the number of mixing units increases, the flow velocity rises, and the fluid undergoes mixing through more layers. With an increase in the number of mixing units, the fluid velocity also increases, leading to more thorough particle mixing and alleviating the initial non-uniform mixing caused by low flow velocity.

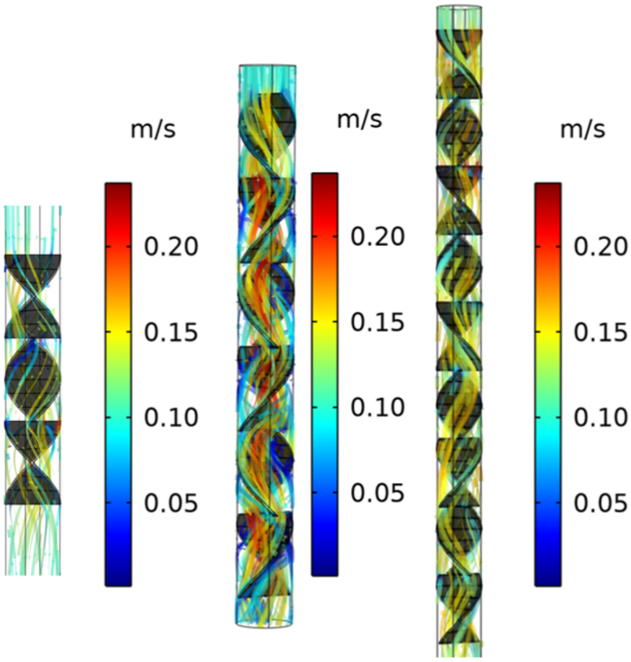

Fig. 10. Streamline diagrams for varying numbers of units

3.3. Numerical simulation of the drop plate mixing process

As shown in Fig. 11, after particles enter the drop plate below from the upper pipe opening, their velocity decreases at the bottom and top of the water layer on the plate. The trailing particles accelerate into the next stage under the influence of the water flow. The velocity in the middle section remains relatively stable, primarily influenced by fluid entrainment. This indicates that the thickness of the water layer formed on the drop plate significantly affects particle flow. It is necessary to control the water flow depth to maintain the particle regulation zone. Appropriate adjustments to the flow velocity and increasing the width of the plate are essential. However, the plate length should not be excessively long to avoid overloading the corner areas and causing particle accumulation.

Under different inclination angles, the velocity distribution does not exhibit significant differences. When the inclination angle is 15 degrees, the fluid flows relatively slowly through the upper - middle section of the drop plate. The corner areas can effectively buffer the fluid - particle mixture, enabling particles to pass through each baffle bar (assuming " Ramp plate " refers to baffle bars; adjust if a more

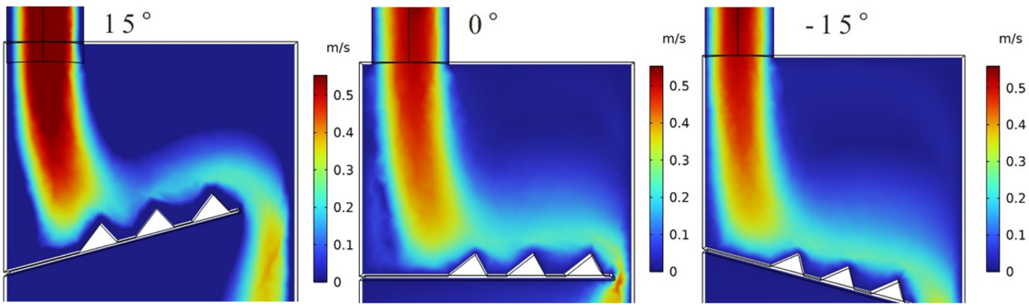

Fig. 11. Drop box velocity distribution cloud

specific term is needed) and thus increasing their utilization rate. When the inclination angle is 0 degrees, the flow velocity of the water layer decreases as it passes through the middle section of the baffle bars, but the influence of the baffle bars on the fluid flow is limited. When the inclination angle is -15 degrees, the contact area between particles and the baffle bars increases, yet the residence time of particles on the baffle bars decreases, resulting in reduced processing efficiency.

4. Test analysis

4.1. Specimen and test methods

4.1.1. Specimen

The coal sample was collected from Zhujixi 13 trough raw coal, crushed and sieved, and the-0.5mm particle fraction was taken. The particle size composition is shown in Table 2. From Table 2, the ash content of the sample is 30.83 %. The proportion of 0.5-0.25 mm grain size is the highest (40.89 %), which is the main grain size of the coal sample; followed by 0.25-0.125 mm (31.29 %), the total proportion of these two fractions is more than 72 %. Fine-grained (⩽ 0.075mm) accounts for a relatively small proportion: 0.075-0.045mm is only 3.75 %, -0.045mm is 10.54 %.

Table 2. Particle size composition of sample

Fraction of grain size /mm	Yield /%	Ash /%	Cumulative yield on sieve /%		Cumulative yield on sieve /%	
			yield /%	ash /%	yield /%	ash /%
0.5-0.25	40.89	32.99	40.89	32.99	100.00	30.83
0.25-0.125	31.29	30.71	72.18	32.00	59.11	29.34
0.125-0.075	13.53	27.07	85.71	31.22	27.82	27.79
0.075-0.045	3.75	23.27	89.46	30.89	14.29	28.48
-0.045	10.54	30.33	100.00	30.83	10.54	30.33
Footing	100.00	30.83				

4.1.2. Test method

The pulp was subjected to a 1.5-liter single-cell flotation machine to adjust the pulp flotation and the jet-pipeline-drop plate pulp conditioning device. Flotation after conditioning in different links of each system was compared to analyze the differences in flotation improvement indicators. Analyze whether each link of Jet Pipeline Drop plate has a certain influence on the flotation quality of pulp properties, and whether the effect of down-regulation of pulp can be significantly improved in each link.

The slurry concentration was 80 g/L, the collector was 1200 g/t n-dodecane, and the foaming agent was 120 g/t methyl isobutyl methanol. The laboratory RK/FD-1.5L single cell flotation machine was used in the flotation test. Flotation setting conditions: impeller speed is 1800 r/min, flotation aeration is 150 L/h, foam collection time is 3min. The clean coal and tail coal products obtained from the test were subjected to filtration, drying, weighing and ash determination. The clean coal yield and clean coal ash were compared, and the recovery rate of clean coal combustibles was calculated as an index to judge the flotation effect. The calculation formula is:

$$\varepsilon_i = \frac{\gamma_i(100-A_i)}{100(100-A_f)} \times 100\% \quad (1)$$

ε_i is the combustible recovery rate of flotation clean coal, γ_i is the yield of clean coal, A_i is the ash content of clean coal, A_f is the ash content of feed.

4.2. Results and analysis

From the flotation test results in Table 3, it can be seen that the ash content of each group is not much different, indicating that the device can normally wash and select clean coal products that meet the ash requirements. Compared with the slurry adjustment effect of 1.5 liter single tank flotation machine, each link of the device has improved the slurry adjustment effect of coal slime. Among them, the increase of jet grouting is the largest, the yield of clean coal is increased by 5.28 %, and the recovery rate of clean coal combustible is increased by 5.82 %. When the jet, pipeline and drop plate work together, the yield of clean coal is increased by 6.85 %, and the recovery rate of clean coal combustible is increased by 8.85 %.

Table 3. Comparative analysis of flotation performance

Testing equipment	Clean coal yielding rate / %	Fine coal ash / %	Calculate the feed ash / %	Recovery of combustible matter
Unit flotation machine	60.55	11.55	34.86	77.46
Jet	65.83	11.64	34.16	83.28
Pipeline mixing	62.55	11.14	34.31	79.76
Jet + Pipeline mixing	66.13	11.04	34.77	84.98
Jet + Drop plate	66.72	11.84	34.82	85.03
Jet + Pipeline mixing + Drop plate	67.4	11.34	34.85	86.31

5. Conclusions

The numerical simulation of the device indicates that when the ratio of the incident flow rate to the instantaneous mixing volume in the tank is 0.414, the distribution of eddy current zones is the densest, with the largest number of small eddies, which is beneficial for mixing. This suggests that the tank has an optimal flow field for the mixing of reagents and pulp. Additionally, as the number of mixing units inside the pipeline mixer increases, the fluid velocity rises, resulting in more thorough particle mixing and alleviating the issue of uneven mixing caused by an initially low flow rate. When the drop plate is set at an inclination angle of 15 degrees, the utilization rate of the fluid passing through the baffle bars is relatively high. However, when the inclination is downward, although the fluid velocity is faster, the particle regulation effect is reduced.

This device can wash clean coal products that meet the ash requirements. Compared with the traditional pulping device, this device has a good pulping effect. Compared with the slurry flotation of 1.5 L single tank flotation machine, the flotation test was carried out on the slurry after the slurry was adjusted by the Jet - Pipeline mixing - Drop plate combined slurry adjustment device. The yield of clean coal was increased by 6.85 %, and the recovery rate of clean coal combustible was increased by 8.85 %.

Acknowledgements

This work was supported by: National Natural Science Foundation of China (Grant No. 52574307), National Natural Science Foundation of China (Grant No：52504282).

References

MA L Q, LI J H, HUANG G, ET AL., *Application of the high-shear pulp conditioning technology and equipment in fine coal flotation process*, Coal Preparation Technology, 2021, (01), 28–32.

XIAO Y, LEI M, LI K J, ET AL., *Experimental Study on Flow Characteristics of Multiple Porous Jets in Crossflow*, Advances in Water Science, 2012, 23(03), 390–395.

CHENG M Z, CAI Y, CHEN L H, ET AL., *Structure design and flow-field simulation of high-pressure water jet nozzle based on CFD*, Journal of Machine Design, 2023, 40(12), 79–85.

YU Y F, LI C X, MENG H B, ET AL., *Jet Flow and Entrainment Characteristics of Nozzles with Different Shapes*, The Chinese Journal of Process Engineering, 2014, 14(04), 549–555.

ZHANG J Z, WEI L J, ZHANG Z H, ET AL., *Influence of Nozzle Structure Based on CFD on Back-propelling Characteristics of High-pressure Water Jet*, Chinese Hydraulics & Pneumatics, 2021, 45(03), 102–107.

WEI T, PENG Y, VINK S., *The joint action of saline water and flotation reagents in stabilizing froth in coal flotation*, International Journal of Mineral Processing, 2016, 148, 15–22.

ZHAO J., *Application of a Novel Flotation Collector in Coal Preparation Plants*, Mining Equipment, 2023, (08), 93–95.

DAI S Q, ZHANG R, LIU Q S, ET AL., *Experimental study on biodiesel collector enhanced coal fly ash flotation decarbonization*, Coal Science and Technology, 2023, 51(S2), 336–343.

QU J Z, LUO C, LI P Y, ET AL., *Advances in Flotation Collectors of Low-rank Coal and Its Interaction Mechanism*, Metal Mine, 2023, (08), 28–35.

WANG C, WANG C, YU A, ET AL., *Effect of closure characteristics of annular jet mixed zone on inspiratory performance and bubble system*, Processes, 2021, 9(8), 1392.

WANG H N, YANG W Q, LI D L, ET AL., *Numerical simulation and experimental study of impact flow enhancing flotation pulp conditioning*, Journal of China Coal Society, 2020, 45(S1), 443–450.

WANG L, JIA Y, YAN X, ET AL., *Gas–liquid numerical simulation on micro-bubble generator and optimization on the nozzle-to-throat spacing*, Asia-Pacific Journal of Chemical Engineering, 2015, 10(6), 893–903.

ZHU Y, CAI W, WEN C, ET AL., *Numerical investigation of geometry parameters for design of high performance ejectors*, Applied Thermal Engineering, 2009, 29(5–6), 898–905.

ANSARI M, BOKHARI H H, TURNEY D E., *Energy efficiency and performance of bubble generating systems*, Chemical Engineering and Processing: Process Intensification, 2018, 125, 44–55.

HAN Y L, WANG X, ZHU J B, ET AL., *Enhancement of coal slurry conditioning flotation using jet-stirring coupling flotation device*, Journal of China University of Mining & Technology, 2023, 52(02), 380–388+416.

XU G, BU X, MAO Y, ET AL., *Combined column and cell flotation process for improving clean coal quality: Laboratory-scale and industry-scale studies*, Energy Sources, Part A: Recovery, Utilization, and Environmental Effects, 2020, 42(21), 2678–2687.

ZHOU W, ZHU J B, MIN F F., *Study on the Hydrodynamic Characteristics of Jet Flotation Machine's Jet Stirring Device*, International Journal of Coal Preparation and Utilization, 2020, 40(11), 780–789.

FENG A A, ZHOU W, ZHU J B, ET AL., *Design and experimental study of the jet-stirring integrated flotation feed pulp preconditioning device*, Coal Preparation Technology, 2018, (05), 67–70.

WANG H, LI D, YANG W, ET AL., *Optimizing oxidized coal flotation using impact flow conditioning pulp*, International Journal of Coal Preparation and Utilization, 2022, 42(8), 2299–2313.

LI D, LIANG Y, WANG H, ET AL., *Effect of slurry preconditioning on the occurrence of major minerals in the flotation products of coal*, International Journal of Coal Preparation and Utilization, 2022, 42(9), 2597–2612.

GAO H, WEI Z K, SHI Y X, ET AL., *Design of the CFD numerical simulation-based bubble generator of jet microbubble flotation cell*, Coal Preparation Technology, 2023, 51(01), 30–37.

ZHENG H X, LUO Y, ZANG J Y, ET AL., *Effect of nozzle outlet type on the flow field velocity and impact pressure of high-pressure water jet peening*, Journal of Fluids Engineering, 2022, 144(7), 071201.